Engineering Chemistry
ISSN: 2813-6535, Vol. 11, pp 7-23
doi:10.4028/p-xbw7Qg

Submitted: 2025-03-24
Revised: 2025-04-24
Accepted: 2025-05-08
Online: 2025-09-10

Citric Acid-Treated Polyethylene-Calcium Carbonate Composites with Tunable Photoluminescence, Porosity, and Adsorption Properties for Oil Contaminants Remediation

Ayodunmomi Esther Olowofoyeku[1,a,*], Ademola Kabiru Aremu[2,b], Abel Olajide Olorunnisola[3,c]

[1]Pan African University Life and Earth Sciences Institute (Including Health and Agriculture), PAULESI, University of Ibadan, Ibadan, Nigeria.

[2]Department of Agriculture and Environmental Engineering, University of Ibadan, Ibadan, Nigeria.

[3]Department of Wood Products Engineering, University of Ibadan, Ibadan, Nigeria.

[a]ayoolowo1122@gmail.com, [b]ademolaomooroye@gmail.com, [c]abelolorunnisola@yahoo.com
Corresponding author: ayoolowo1122@gmail.com

Keywords: Photoluminescent polymers, porous composites, calcium carbonate, oleic acid, citric acid, oil contaminant.

Abstract. Oil contamination from petroleum hydrocarbons and other sources poses significant environmental and health risks due to its persistence and toxicity. This study developed polyethylene-calcium carbonate (PE-CC) composites with tailored structural and surface properties to enhance oil adsorption. The composites were fabricated through melt blending (PE:CC = 40:60), with the calcium carbonate (CC) filler first modified using oleic acid (OA) (0, 0.5, and 1.5 wt.%) to improve hydrophobicity and dispersion, followed by citric acid (1 M) treatment of the composites to induce porosity and optimize oil adsorption. X-ray diffraction (XRD) and Fourier-transform infrared spectroscopy (FTIR) confirmed successful surface modification of CC, as evidenced by reduced diffraction peak intensities and the emergence of new functional groups at 2970 cm^{-1} and 1395.12 cm^{-1}. Citric acid treatment led to partial CC dissolution, resulting in up to 8.96 % weight loss, as confirmed by XRD and energy-dispersive spectroscopy (EDS). Scanning electron microscopy (SEM) revealed increased porosity (up to 40 μm) and enhanced surface roughness, particularly in TE 3. Wettability analysis demonstrated a maximum contact angle of 160.80° following OA modification of CC, while oil adsorption tests of the PE-CC composites showed substantial improvements in oil uptake, with vegetable oil adsorption increasing from 5.21 % (NE) to 18.75 % (TE 3), and hexane and diesel reaching 18.4 % and 12.5 % respectively, in TE 3. Photoluminescence analysis revealed wavelength-dependent blue-violet emissions with broad peaks at 405 and 570 nm when excited at 255 and 405 nm, respectively, indicating potential optical applications. These findings show the potential of OA and citric acid modifications in enhancing the surface properties, photoluminescence, and adsorption efficiency of PE-CC composites, positioning them as promising candidates for oil remediation and multifunctional industrial applications.

Introduction

Oil contamination from petroleum hydrocarbons, industrial lubricants, and vegetable oils poses significant environmental and health risks due to its persistence and widespread occurrence [1, 2]. These pollutants infiltrate water, soil, and air through spills, runoff, and improper disposal, leading to oxygen depletion in aquatic ecosystems, groundwater contamination, and inhibition of plant growth and development. Their hydrophobic nature limits natural biodegradation, causing bioaccumulation and toxicity, with petroleum-based compounds exhibiting potential carcinogenic effects [3]. Addressing this challenge requires materials that adsorb oil efficiently and also retain their structural integrity.

Polymer-based composites have emerged as promising materials for oil remediation due to their tunable surface properties, chemical resistance, and ability to incorporate hydrophobic reinforcements that enhance oil uptake [4]. By leveraging the complementary properties of their constituents, polymer composites offer enhanced mechanical strength, thermal stability, and controlled wettability, making them suitable for oil spill recovery and environmental applications [5-7]. Beyond their core structural properties, advanced composites can also incorporate multifunctional characteristics such as photoluminescence, electrical conductivity, and self-healing capabilities, broadening their utility in areas like sensor technology, renewable energy, and biomedicine [7-10].

Among polymer composites, polyethylene (PE)-based systems reinforced with calcium carbonate (CC) have gained attention for their improved mechanical, thermal, and barrier properties. CC, a widely used mineral filler, enhances the dimensional stability and density of PE composites while influencing water adsorption, dispersion, and swelling behavior [11-14]. A comparative study indicated that CC improves crystallinity and processability in high-density polyethylene (HDPE) composites more effectively than alternative fillers like eggshells [11]. However, its hydrophilic nature hinders dispersion in hydrophobic polymer matrices, leading to agglomeration and weak filler-matrix bonding, which can compromise mechanical integrity and reduce efficiency in oil adsorption applications [15, 16].

To address this limitation, surface modification of CC with hydrophobic agents such as oleic acid (OA) has been explored to improve its compatibility with polymer matrices. OA-treated CC enhances interfacial adhesion, increases composite durability, and improves oil uptake by reducing surface energy mismatch [17-19]. Additionally, acid treatments, such as nitric or sulfuric acid, modify polymer surfaces by introducing functional groups, increasing roughness, and enhancing adsorption properties. For instance, nitric acid treatment has been shown to introduce nitro groups onto styrofoam, creating an anionic surface capable of adsorbing Pb^{2+} ions effectively [20]. However, strong acids can also degrade polymer mechanical properties, necessitating careful selection of modification strategies [20]. Citric acid is a mild, biodegradable organic acid that can selectively reacts with calcium carbonate fillers to produce CO_2 without damaging the polymer matrix, unlike stronger acids such as nitric acid. Also, it is safer and eco-friendly making it ideal for sustainable material processing and green chemistry applications [21].

Beyond structural modifications, functional enhancements such as photoluminescence can add value to oil-remediating materials, particularly for real-time monitoring and detection of contaminants. While neither PE nor CC exhibits significant intrinsic photoluminescence, composite formulations incorporating luminescent fillers or surface-modified CC may develop unique optical properties. Fu et al. demonstrated that CC enhanced photoluminescence in alginate by releasing Ca^{2+} ions, which altered structural morphology and facilitated electron transfer, offering a sustainable alternative to rare-earth-based materials [22]. These findings suggest that incorporating modified CC into PE composites could yield new functionalities beyond oil adsorption, making them applicable in environmental sensing technologies.

While studies have explored OA-treated CC for improved polymer compatibility, the role of acid-induced porosity from CC dissolution in enhancing oil adsorption and photoluminescence remains unexamined. This study investigates the influence of OA-modified CC and citric acid-induced porosity on polyethylene-calcium carbonate composites (PE-CC), focusing on structural and surface properties, wettability, oil adsorption, hardness, and photoluminescent behavior. By addressing these aspects, this research aims to develop advanced polymer composites with optimized oil-remediating capabilities and potential multifunctionality.

Materials and Methods

Materials

The primary materials used in this study were Low-Density Polyethylene pellets (PE) and calcium carbonate (CC). The PE pellets used were commercially available industrial-grade material with a melt flow rate of 2.5 g/10 min (ASTM D1238, 190 °C/2.16 kg, ≥ 99% purity, Shijiazhuang Jintaichang New Materials Co., Ltd., China). The calcium carbonate used was also commercially available industrial grade (10 µm, 98 % purity, local supplier, Nigeria). Oleic acid (99 % purity, Sigma-Aldrich, Germany) and citric acid (99.5 % purity, Sigma-Aldrich, Germany) were used as chemical modifiers. Ethanol (96 % v/v, Sigma-Aldrich, Germany) was employed as the solvent for OA treatment, and laboratory-produced distilled water was used for preparing solutions and for rinsing after citric acid modification.

Preparation of OA-treated CC

OA was dispersed in 100 mL of ethanol at the desired concentrations of 0, 0.50, and 1.50 wt.%. To this solution, 100 g of CC was added with continuous stirring for 3 h to ensure uniform dispersion of OA on the surface of the CC particles. The mixture was then heated to dryness while stirring at 70 °C for a period of 3 h to ensure complete removal of the solvent. The resulting powder was pulverized and labeled as follows based on the OA content: CC1 (0 wt.% OA), CC2 (0.50 wt.% OA), CC3 (1.50 wt.% OA). These powders were then stored for subsequent use in the fabrication of polymer nanocomposites [23]. The wettability of the CCs was assessed by measuring the contact angle of a water droplet on their surface using a Drop Shape Analyzer (DSA30, Krüss). Higher contact angles signify greater hydrophobicity and a reduced attraction to water [24].

PE-Composite fabrication

PE-CC composites were fabricated using the melt blend method. The CC samples (CC1, CC2, and CC3) were incorporated into PE at a CC weight fraction of 60 % to produce the polymer composites, labeled as follows: NE 1 (CC1 with 0 wt.% OA), NE 2 (CC2 with 0.50 wt.% OA), NE 3 (CC3 with 1.50 wt.% OA). The blend was processed using a twin-screw extruder maintained at 120 °C with a screw speed of 100 rpm for 10 min to ensure uniform CC dispersion within the polymer matrix. The extrudate was then pressed into films of appropriate thickness using a Rositek heat press with a pressure of 500 MPa for 5 min (RMP2, USA) and cut based on the test standard. Pure PE was processed using the same method and labeled as NE to serve as a reference material for comparison against the composite samples [25]. Their wettability was assessed using the same procedure applied to the OA-treated CCs.

Synthesis of porous polymer-composites

The PE-CC composites were made porous by immersion in excess citric acid. Specifically, 20 pieces of 10 mm x 10 mm x 2 mm of each composite (NE 1, NE 2, and NE 3) were immersed in 50 mL of 1 M citric acid solution for 48 h. After immersion, the composites were removed, rinsed three times with distilled water, and dried at 35 °C for 12 h. The citric acid-treated composites were labeled as: TE 1 (from NE 1), TE 2 (from NE 2), and TE 3 (from NE 3). Pure PE treated with citric acid was labeled as TE [20]. Weight loss was calculated using Eq. 1.

$$\text{Weight loss } (\%) = \frac{w_1 - w_0}{w_0} \times 100 \quad (1)$$

where w_0 represents the initial weight of the composite before citric acid treatment (in grams) and w_1, the final weight of the composite after citric acid treatment (in grams).

Crystallographic analysis

The crystalline structure of the CC samples, PE, and the polymer composites was analyzed using a Malvern Panalytical Empyrean X-ray diffractometer equipped with Cu-Kα radiation (λ = 1.5406 Å). Data were collected in the 2θ range of 10° – 80°, with a scan rate of 0.026°/s. Diffraction patterns of the CCs were matched against the ICDD reference database to determine its crystalline phases.

Morphological analysis

Surface morphology, particle dispersion, and associated changes were analyzed using a Philips XL30 ESEM at a magnification of 600x. Elemental composition was determined using Energy Dispersive X-ray Spectroscopy (EDS) integrated with the Philips XL30 ESEM. Surface profiles and roughness parameters of the composites were analyzed using Gwyddion 2.45 software.

Functional groups

Functional group analysis on the CCs and polymer composites was performed using an FTIR spectrometer PerkinElmer Spectrum Two in the wavenumber range of 4000–600 cm^{-1}. Samples were analyzed using the attenuated total reflectance (ATR) method for the CC and their composites.

Photoluminescence spectroscopy

The photoluminescent properties of the PE composites were evaluated using an RF-6000 Shimadzu Spectro fluorophotometer. Emission spectra were recorded at excitation wavelengths of 255 nm and 405 nm to evaluate how CC and citric acid treatments influence the luminescent properties of the polymer composites. Also, NE 3 and TE 3 were subjected to 10 cycles of UV exposure at a wavelength of 255 nm for 5 minutes per cycle, separated by 1 h in darkness [26]. After each cycle, the emission spectra were evaluated as a percentage of the original intensity to determine photoluminescence stability.

Shore hardness of polymer composites

The Shore D hardness of the polymer composites was measured using a durometer in Shore Hardness Units (S.H.U.), following ASTM D2240 standards [27]. Samples measuring 50 mm by 50 mm with a thickness of 2 mm were placed on a flat surface. The durometer's indenter was pressed perpendicularly onto each sample for 10 s to stabilize the reading. Three measurements were taken at different locations on each sample to account for surface variability, and the average was recorded as the final hardness value.

Adsorption test

The oil adsorption test was conducted following the ASTM D570 standard for water adsorption [28]. The test was designed to evaluate and compare the adsorption capacities of the PE-CC composites for various non-polar liquids, including vegetable oil, n-hexane, and diesel. Water was used as a benchmark. Uniform samples of 10 mm by 10 mm and 2 mm thickness were weighed to determine their dry weight (W_0). They were then immersed in the respective liquids at 25 ± 1 °C for 24 h in sealed containers to prevent evaporation. After immersion, the samples were removed, gently wiped to remove excess liquid, and reweighed (W_1). Each test was performed in triplicate to ensure reproducibility and average values with standard deviations were reported. Adsorption capacity was calculated using the formula in Eq. 2.

$$\text{Adsorption Capacity (\%)} = \frac{W_1 - W_0}{W_0} \times 100 \quad (2)$$

Statistical analysis

All measurements were performed in triplicate, with results expressed as mean ± standard deviation (SD). Differences between sample groups were analyzed using ANOVA, followed by Dunnett's multiple comparison test, with statistical significance set at $p < 0.05$. These statistical methods were chosen to assess the significance of variations in results obtained among the different composite formulations. Identifying statistically significant differences will confirm whether the combined effects of oleic acid treatment and citric acid-induced porosity contribute to improved functional properties. Statistical analysis was conducted using GraphPad Prism 8.

Results and Discussion

Wettability of the OA-treated CC

Surface modification of CC with OA, which was assessed through contact angle, improved its hydrophobicity, as shown in Fig. 1, and was consistent with those reported by Longkaew et al. [29], Al-Shirawi et al. [30], and Wang et al. [24]. Contact angles above 90°, as observed for CC2 and CC3, confirm the hydrophobic nature of the treated CC surfaces, improving their compatibility with nonpolar matrices and reducing moisture uptake. In contrast, contact angles below 90°, as seen in CC1, suggest more hydrophilic behavior and reduced effectiveness in nonpolar composite applications [31].

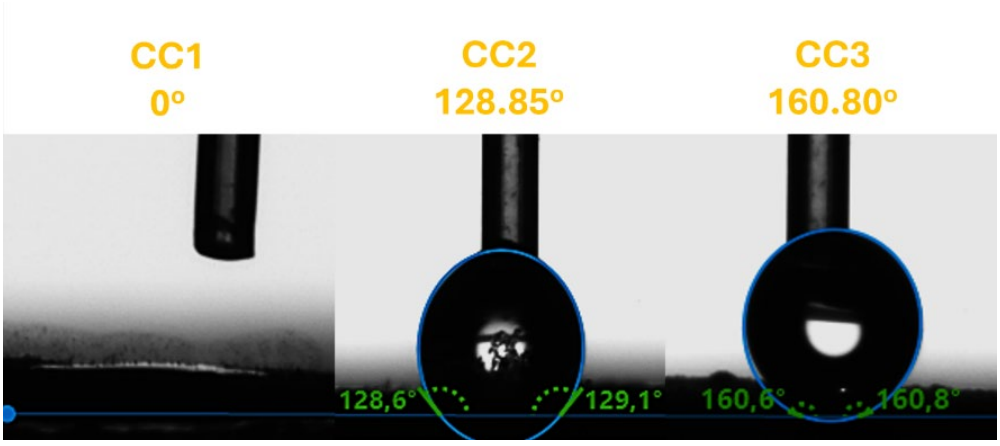

Fig. 1. Contact angles of calcium carbonate fillers after treatment with varying concentrations of oleic acid.

Weight loss due to citric acid treatment

The weight loss of the sample due to citric acid treatment exhibited a clear trend associated with CC dissolution during the citric acid treatment, as presented in Table 1. Pure PE (NE) showed minimal weight loss of just 0.01 %, verifying its stability. However, composites containing CC (NE 1, NE 2, and NE 3) experienced statistically significant weight loss, ranging from 7.84 % to 8.96 % compared to the NE ($p < 0.0001$). The standard deviation values (0.54, 0.23, and 0.16) reflect slight variability in weight loss across the samples, with NE 1 exhibiting the highest deviation, likely due to variations in CC dispersion within the composites. The weight loss trends in composites with mixed phases suggest that the dispersion of CC particles influences the extent of dissolution. More homogeneous dispersion may lead to uniform dissolution during acid exposure, ultimately affecting the material's stability and performance. The balanced chemical equation describing CC dissolution during citric acid treatment is shown in Eq. 3.

$$3CaCO_3 + 2C_6H_8O_7 \rightarrow Ca_3(C_6H_5O_7)_2 + 3CO_2 + 3H_2O \quad (3)$$

During this reaction, CO_2 escapes, reducing the material's overall mass. Rinsing with distilled water further removes the loosely bound insoluble calcium citrate, contributing to weight loss. These two events explain the observed mass reduction after citric acid treatment. These findings align with the substantial weight loss reported for glass-ionomer cement under acid treatment, in contrast to the minimal loss observed in resin composites in a comparative study [32].

Table 1. Filler composition, filler-to-polymer ratio, and weight loss after citric acid treatment of composite samples.

Sample	Filler	Filler OA treatment (%)	Filler to Polyethylene ratio	Weight Loss after citric acid treatment (%)	Corresponding citric acid-treated sample
NE	--	--	0:100	0.01 ± 0.01	TE
NE1	CC1	0.00	60:40	8.96 ± 0.54	TE 1
NE2	CC2	0.50	60:40	7.88 ± 0.23	TE 2
NE3	CC3	1.50	60:40	7.84 ± 0.16	TE 3

Crystalline structure of CC and composites

X-ray diffraction analysis revealed the characteristic structures of PE and CC [33-35]. The XRD patterns of the OA-treated CC fillers, shown in Fig. 2a, were in the monoclinic phase and matched the ICDD card 01-070-0095. The prominent peaks and their matching planes were identified at 2θ = 29.73° (200), 36.31° (020), 39.81° (211), and 43.57° (202). The treatment of CC with OA resulted in a progressive reduction in the intensity of these peaks with increasing OA concentration, aligning with previous studies [36]. This reduction suggests that OA-induced surface modifications altered the diffraction intensity without forming a new crystalline phase. For the pure PE samples (NE and TE) shown in Fig. 2b, the XRD analysis revealed characteristic diffraction peaks at 2θ = 21.86° and 24.26°, corresponding to the (110) and (200) planes of the orthorhombic PE crystalline phase. These peaks were sharp and intense in NE, indicating high crystallinity. However, a slight reduction in the intensity of the (200) plane at 24.26° was observed in the citric acid-treated sample (TE). This suggests a minimal impact of citric acid on the crystalline regions of the PE and the polymer's resistance to acid treatment [33, 37]. In the PE-CC composites (NE 1, NE 2, NE 3, TE 1, TE 2, TE 3), peaks corresponding to both PE and CC were observed, confirming that no chemical interaction occurred during the compositing process (Fig. 2b). In the composites, NE 1, NE 2, and NE 3, the PE peaks at 2θ = 21.86° and 24.26° were significantly diminished, due to the dominant intensity of the CC peaks [38]. Following citric acid treatment (TE 1, TE 2, TE 3), the PE peaks became slightly pronounced, while the CC peaks showed a reduction in intensity. This reduction in CC peak intensity in the citric acid-treated composites confirms partial dissolution of CC during citric acid treatment. Despite these changes, the PE peaks remained discernible across all composites, suggesting that the polymer maintained its structural integrity within the matrix. The OA coating on CC appeared to have minimal impact on the XRD patterns of the composites, both before and after citric acid treatment. This observation indicates that while OA altered the surface properties of CC, it did not significantly affect the crystalline structures of the composite materials [39]. These findings indicate that while OA modifies surface properties, it does not induce significant crystalline phase changes, which is essential for maintaining mechanical stability in composite applications.

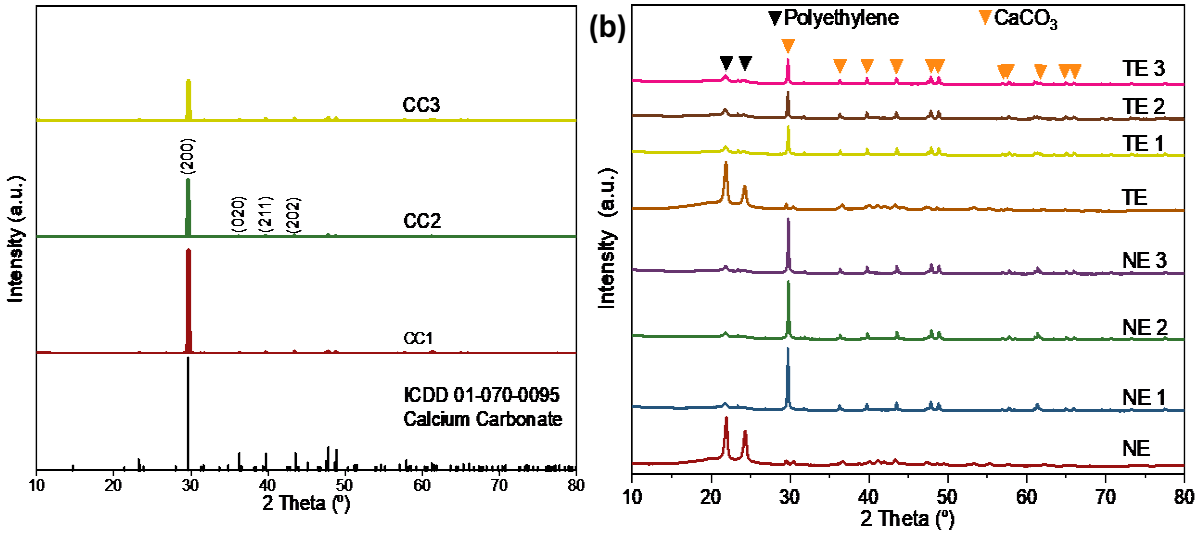

Fig. 2. X-ray diffractograms of the OA-treated CC (a), and the PE-CC composites (b).

Effect of OA and citric acid treatment on the functional groups of CC and composites

The FTIR spectrum (Fig. 3a) of the CC sample CC1 showed characteristic peaks at 1395.12 cm^{-1}, 870.26 cm^{-1}, and 711.98 cm^{-1}. These corresponded to CO_3^{2-} stretching, out-of-plane bending, and in-plane bending vibrations, respectively, as have been reported by other authors [11, 29, 34]. In the OA-treated CC samples (CC2 and CC3), additional peaks appeared around 2970 cm^{-1}, representing CH_2 stretching vibrations. Also, the peaks at 1395.12 cm^{-1} and 870.26 cm^{-1} exhibited increased intensity as the OA concentration increased, aligning with surface modifications of the CC particles [36]. The FTIR spectra of the pure PE samples presented in Fig. 3b show characteristic adsorption bands associated with PE [23, 36]. These include symmetric and asymmetric stretching vibrations of CH_2 groups at approximately 2915 cm^{-1} and 2849 cm^{-1}, as well as bending vibrations around 1465 cm^{-1} and 719 cm^{-1}.

Furthermore, the PE-CC composites (NE 1, NE 2, NE 3, TE 1, TE 2, and TE 3) had additional peaks corresponding to CC (Fig. 3b). These include CO_3^{2-} peaks at 1395 cm^{-1} and 870 cm^{-1}, while the expected peak at 1395 cm^{-1} was merged with the CH_2 bending peak at 1465 cm^{-1}. In the citric acid-treated composites, a reduction in the intensity of the carbonate peaks at 1395 and 870 cm^{-1} was observed, confirming partial carbonate loss due to the treatment.

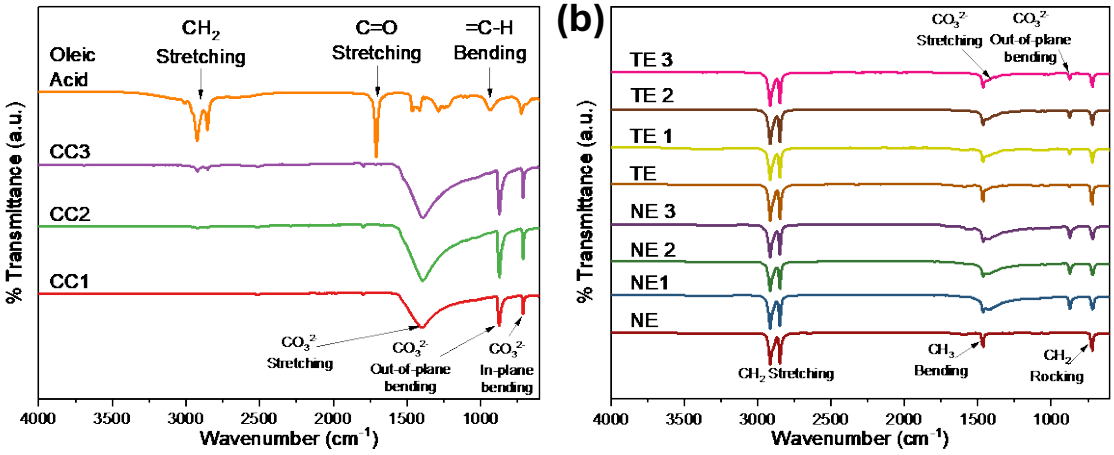

Fig. 3. FTIR spectra of the OA-treated CC (a), and the PE-CC composites (b).

Morphological changes after oleic and citric acid treatment

The SEM micrographs shown in Fig. 4a reveal the morphological differences across the samples particularly before and after citric acid modification. The surface of non-treated pure PE (NE) appeared smooth and continuous [24, 40]. However, in the acid-treated PE (TE), surface irregularities, undulations, and sharper edges were observed. These changes were attributed to localized stress, strain, or minor oxidative effects, particularly in amorphous regions of the polymer during citric acid treatment. In the composites, the incorporation of CC introduced various sizes of CC particles (up to about 40 μm) within the polymer matrix which were well-distributed. Unlike the findings of Ritonga et al. [36], moderate agglomeration was observed in the fillers, likely due to heating to dryness of the CC fillers during OA treatment. TE 1 and TE 3 displayed significant porosity, characterized by irregular voids, cavities, and surface undulations. These features are attributed to the partial dissolution of CC by its reaction to citric acid. TE 3, being a malleable composite due to the softening effect of OA treatment and the agglomeration of its fillers, exhibited larger pores, more irregular voids, and greater surface undulations than TE 1.

Changes in elemental composition after oleic and citric acid treatment

The differences in elemental composition observed in EDS results were influenced by CC filler and chemical treatments as shown in Fig. 4b. In NE, the spectra showed a strong carbon peak (C-Kα) at approximately 0.277 keV while in NE 1 and NE 3, prominent calcium and oxygen peaks (Ca-Kα) at 3.69 keV and 0.525 keV were observed respectively, confirming the presence of CC. Upon OA treatment of CC in NE 3, the oxygen peak intensity slightly increased. After citric acid treatment, traces of oxygen were detected in pure PE samples (TE), likely from citric acid residues. In TE 1 and TE 3, the calcium and oxygen peak intensities were lower than in untreated samples, indicating partial CC removal.

Effect of CC Fillers and Acid Treatments on the Surface Roughness of Composites

The surface profiles of the materials (Fig. 4c) and their respective roughness parameters (Table 2) support the trends observed in the SEM micrographs. NE had the smoothest surface with the lowest RMS roughness (92.26 nm) and mean roughness (68.38 nm), reflecting its uniform morphology. Adding CC fillers in NE 1 and NE 3 increased surface roughness, with NE 3 showing a higher RMS roughness (183.80 nm) than NE 1 (160.86 nm) due to more heterogeneous surfaces and larger particle aggregations in NE 3 [41]. Citric acid-treated composites (TE 1 and TE 3) had lower roughness values than their untreated counterparts, due to the ‘smoothing effect’ of citric acid treatment. TE 3 exhibited larger pores (over 40 μm) and moderate RMS roughness (136.30 nm), suggesting structural changes that may improve adhesion, wettability, and oil adsorption capacity.

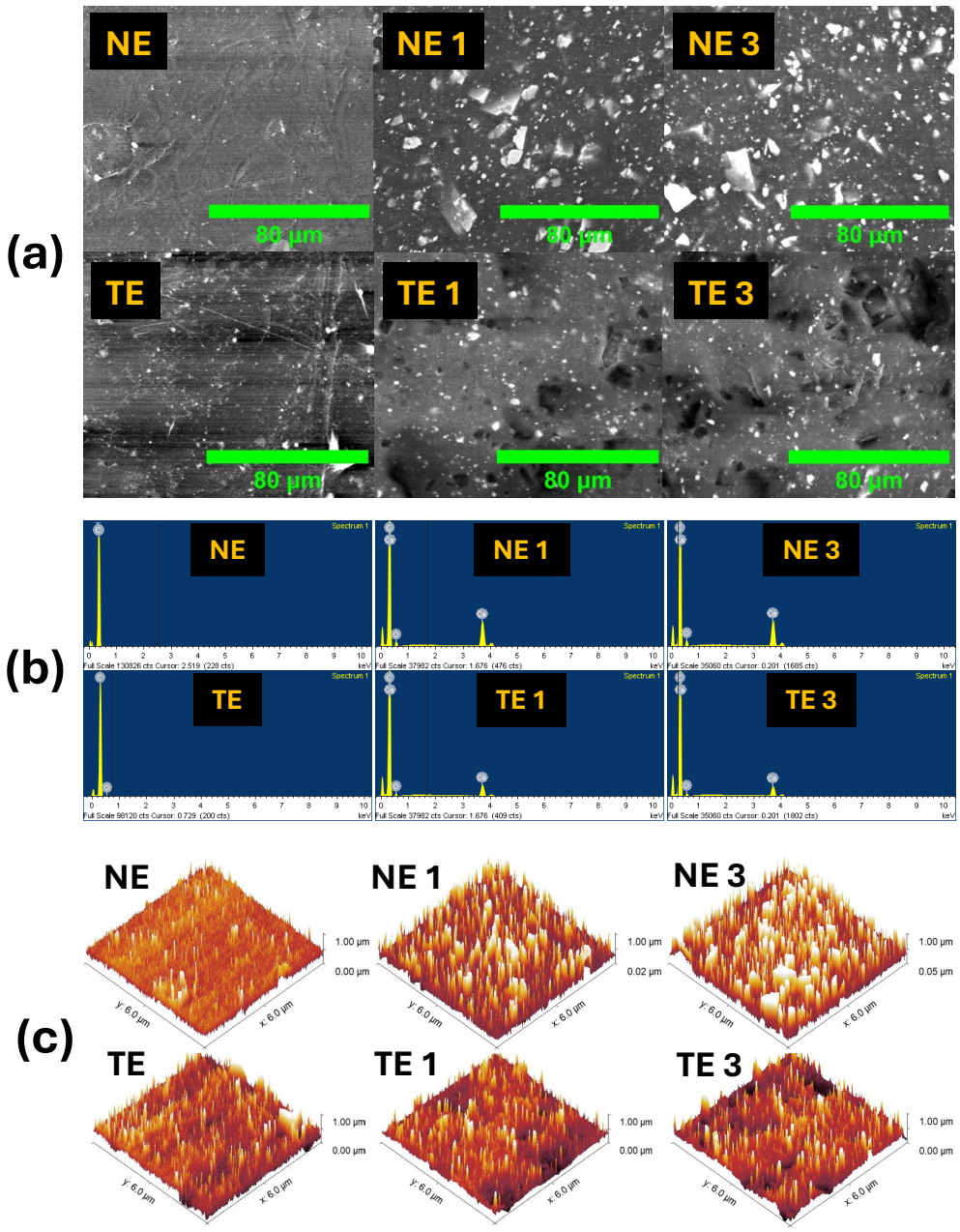

Fig. 4. SEM micrographs (a), EDS analysis (b), and surface roughness mapping (c) of the PE-CC composites.

Table 2. Surface roughness parameters of the PE-CC composites.

Sample	RMS Roughness (Sq)	Mean Roughness (Sa)	Maximum Peak Height (Sp)	Maximum Pit Depth (Sv)
NE	92.2639 nm	68.3794 nm	0.567499 µm	0.432501 µm
TE	144.529 nm	103.551 nm	0.678620 µm	0.321380 µm
NE1	160.855 nm	110.089 nm	0.635592 µm	0.344801 µm
TE1	125.837 nm	89.235 nm	0.647850 µm	0.352150 µm
NE3	183.804 nm	127.822 nm	0.567461 µm	0.385481 µm
TE3	136.301 nm	97.405 nm	0.656183 µm	0.343817 µm

Photoluminescent properties of the PE-CC composites

The impact of citric acid treatment and CC surface modification on the photoluminescent properties of the composites was evaluated to determine how morphological and structural changes influence light emission. The photoluminescence (PL) spectra of PE and PE-CC composites when excited at 255 nm and 405 nm are displayed in Fig. 5A1 and Fig. 5B1. The characteristic broad emissions recorded are similar to those of polymeric materials in other similar studies [42, 43]. Generally, as the excitation wavelength increased, luminescence peaks shifted and narrowed demonstrating a wavelength-dependent emission behavior (Tareeva et al. 2020). The observed photoluminescence trends, including spectral shifts, changes in emission intensity, and peak narrowing, were attributed to surface defects and structural modifications introduced by citric acid treatment and the incorporation of OA-modified CC fillers in the polymer. At 255 nm excitation, all materials exhibited broad emissions at 405 nm, with the non-porous composites (NE 1, NE 2, NE 3) showing a broadening and slight shift toward higher emission wavelengths. In contrast, the porous citric acid-treated materials exhibited narrower emission peaks. Changes in pure PE were attributed to surface modifications and tension release, while in composites, OA-modified filler and citric acid-induced porosity influenced their luminescent properties. At 405 nm excitation, the observed broad emissions were centered around 570 nm, with untreated PE exhibiting lower intensity than treated PE, suggesting the formation of surface defects. Non-porous composites had higher intensity than their porous counterparts, suggesting that porosity negatively impacts PL. The CIE chromaticity diagrams (Fig. 5A2 and Fig. 5B2) further confirm a shift towards fainter violet in composites at 255 nm excitation, while excitation at 405 nm shows a cluster around the violet region, with NE 3 and TE 3 shifting to the yellow-green region, demonstrating tunable photoluminescent properties. The reduction in PL intensity in porous samples may be attributed to increased surface scattering and non-radiative recombination centers formed due to structural defects introduced by citric acid treatment. The samples NE 3 and TE 3 demonstrated notable photoluminescent stability, as illustrated in Fig. 6a and Fig. 6b. Overall, the structural modifications that enhance photoluminescence, such as altered surface states and functional group interactions, also contribute to the adsorption performance by affecting the material's wettability and porosity. This dual influence underscores the interplay between optical properties and surface activity.

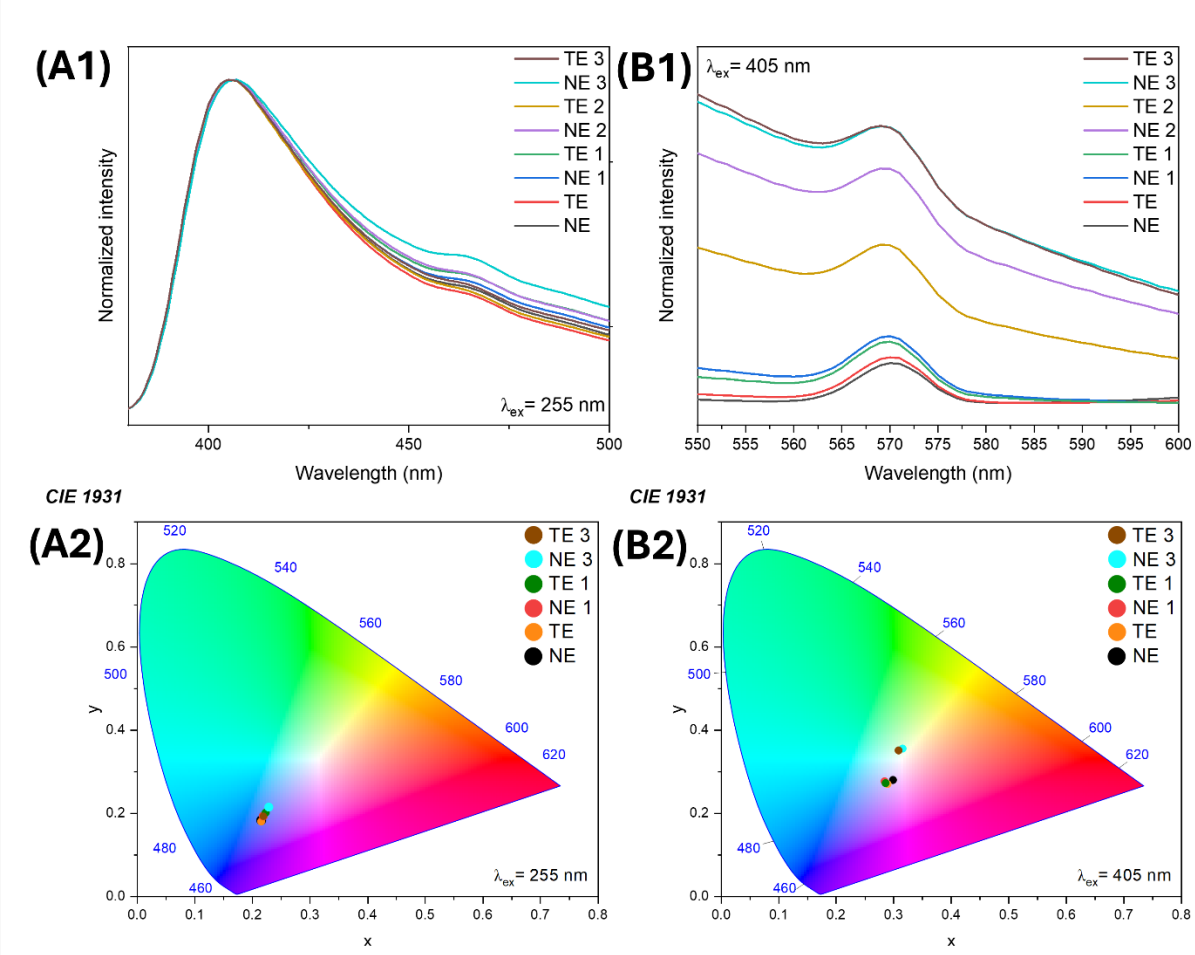

Fig. 5. Photoluminescence spectra of the PE-CC composites at 255 nm (A1) and 405 nm (B1), along with the corresponding CIE chromaticity diagrams at 255 nm (A2) and 405 nm (B2).

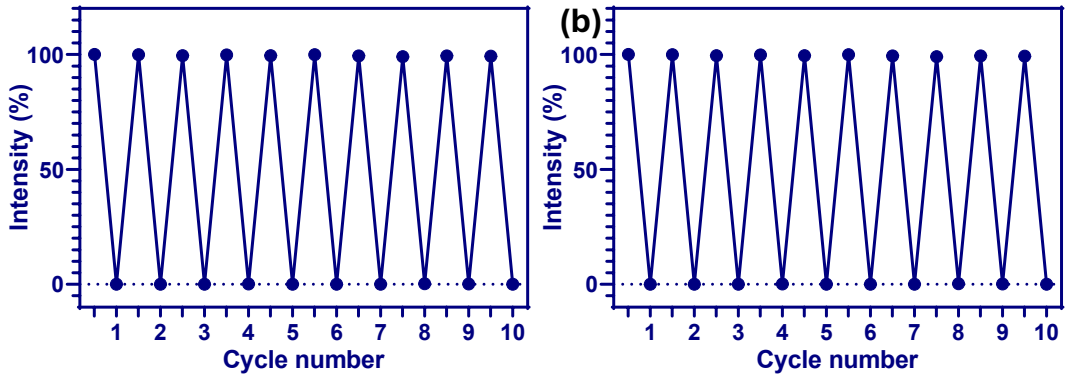

Fig. 6. Photoluminescent stability of the PE-CC composites at 255 nm: NE 3 (a) and TE 3 (b).

Oil affinity and adsorption performance

The oil affinity test result (Fig. 7a) and its statistical analysis (Table 3) reveal the effect of the oil type and sample modifications on adsorption performance. Polymers are inherently hydrophobic, and incorporating OA-treated fillers enhances this property by improving compatibility within the polymer matrix [44]. Treating the composite with citric acid introduces porosity by creating micropores (up to 40 μm) through its reaction with calcium carbonate, increasing the surface area and enhancing contaminant adsorption [21]. This combination of hydrophobicity and increased surface area makes the material more effective for capturing and retaining hydrophobic pollutants. The results indicated that water adsorption remains minimal in samples, consistent with PE's hydrophobicity, but increases significantly in the composites and after acid treatment (up to 6.8 % in

TE 1) due to enhanced hydrophilicity and porosity as reported by Jiao et al. (Jiao et al. 2023). Vegetable oil adsorption increased modestly from 5.21 % in NE to 18.75 % in TE 3, due to the fillers' hydrophobic OA treatment and citric acid-induced porosity. Jahani et al. also observed a similar trend in studies on dye-absorbent materials incorporating hydrophobic modifications [45]. Hexane and diesel followed similar patterns, with TE 3 achieving maximum adsorption (18.4 % and 12.5 % respectively), reflecting improved affinity for both polar and non-polar liquids. Statistical analysis showed that liquid type and sample modifications significantly affected adsorption, accounting for 23.05 % and 56.25 % of the variance, respectively, with their interaction contributing an additional 20.19 %. Dunnett's test showed significant differences across all comparisons ($P < 0.001$). In practical applications, optimal adsorption occurs when the material matches the liquid, particularly in areas like oil spill remediation or filtration, as their interaction significantly influences adsorption properties and performance. The low standard deviations among replicates indicate consistent structural changes and reliable performance across tests.

Table 3. ANOVA summary results for the liquid adsorption tests.

Source of Variation	Degrees of Freedom	Sum of Squares	Mean Square	F-value	P-value	Variance Contribution (%)
Liquid type	3	457.5	152.5	975.37	< 0.0001	23.05
Sample	7	1116	159.5	1020.16	< 0.0001	56.25
Interaction (Liquid x Sample)	21	400.8	19.09	122.08	< 0.0001	20.19
Residual (Error)	64	10.01	0.1563	-	-	-
Total	95	1985	-	-	-	100

Shore hardness and wettability of the PE-CC composites

The Shore hardness values, shown in Fig. 7b, reveal the effects of modifications on the material's rigidity. Pure PE (NE) had a baseline hardness of 55.6, with minimal deviation whereas a previous study reported 63.9 [46]. Citric acid treatment (TE) slightly reduced the hardness to 55.2, with better consistency. CC reinforcement in NE 1 significantly increased hardness (64.4) (Hayeemasae and Ismail 2021), but citric acid-treated TE 1 (62.1) showed better consistency although Wierzbicka et al. [46] reported reduced Shore values when hexagon boron nitride was added alone but higher values when hexagon boron nitride and titanium were incorporated into PE. Similar trends were observed in NE 2 and TE 2, with TE 2 exhibiting reduced hardness. NE 3 and TE 3 displayed further reductions, indicating an increase in ductility and malleability to OA concentration and porosity (Ippolito et al. 2020). The statistical analysis shows significant differences in the hardness values ($F = 25.90$, $P < 0.0001$) with a strong data fit ($R^2 = 0.9189$). Dunnett's test highlighted significant differences in the comparison of NE against the other untreated and citric acid-treated composites (NE 2, NE 3, and TE 3), while NE vs. NE 1, NE vs. TE 1, and NE vs. TE 2 showed no significant differences. These results indicate that untreated composites are more rigid, while citric acid-treated materials are less rigid and better suited for applications requiring flexibility, porosity, and roughness.

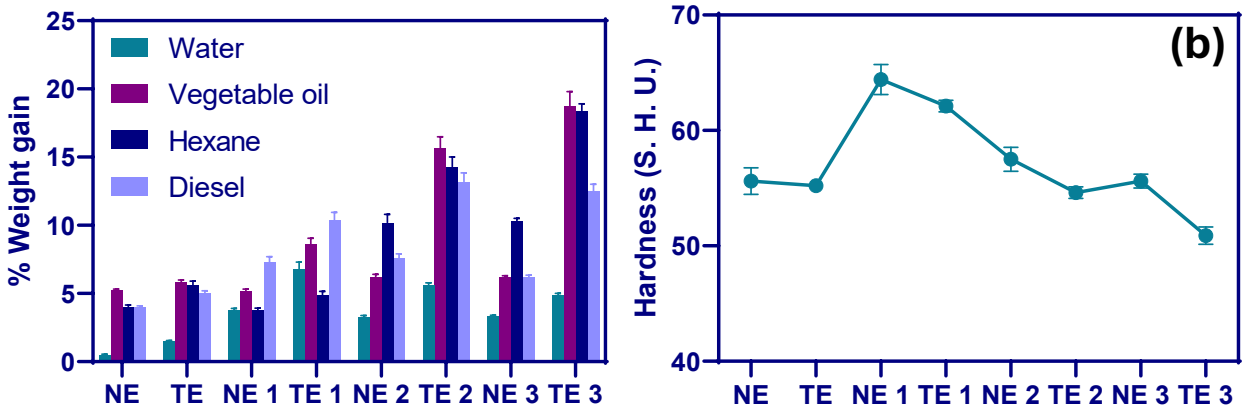

Fig. 7. Oil adsorption capacity (a) and Shore hardness values (b) of the PE-CC composites.

The wettability of the materials was assessed using contact angle measurements, as shown in Fig. 8. The NE samples showed higher contact angles (96.65°, 84.50°, 94.35°), reflecting their hydrophobic surfaces and limited water affinity [47]. In contrast, the TE samples had lower contact angles (90.55°, 64.60°, 74.10°), indicating that citric acid treatment increased surface porosity and made the surfaces more hydrophilic. Additionally, the presence of oleic acid in NE 3 and TE 3 contributed to higher hydrophobicity compared to NE 1 and TE 1. These results show that surface chemistry and porosity influence the water interaction behavior of the composites.

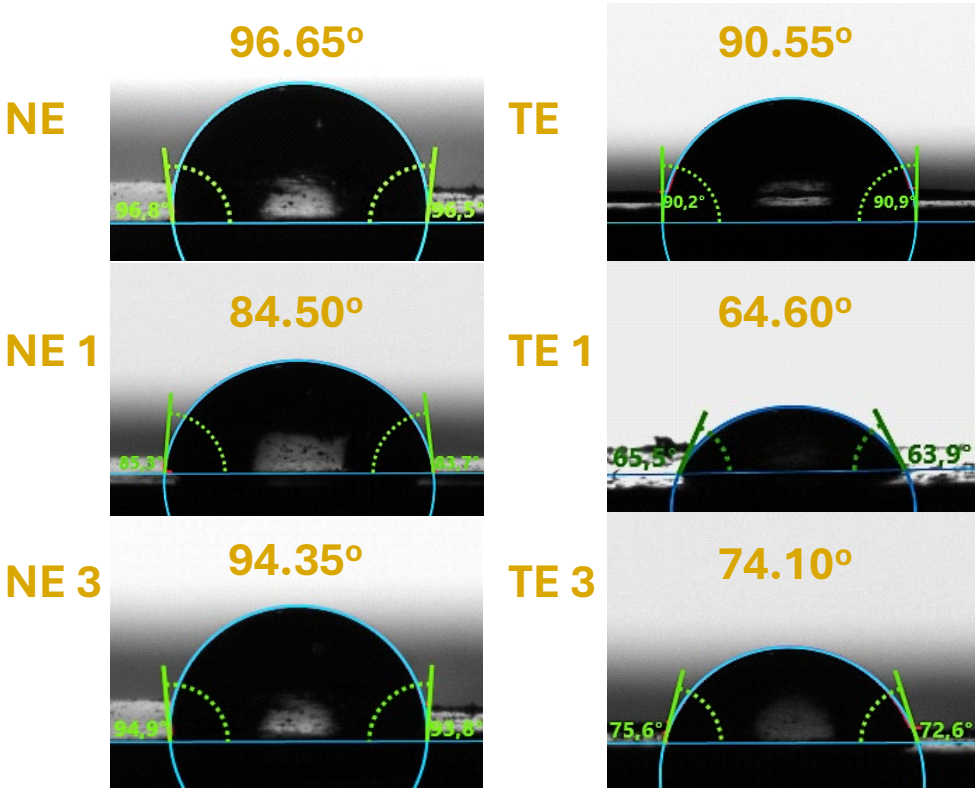

Fig. 8. Contact angles of the PE-CC composites before and after citric acid treatment.

The surface modifications introduced by oleic acid and citric acid treatments have profoundly impacted the properties of the polyethylene-calcium carbonate composites. Citric acid treatment enhanced porosity and surface hydrophilicity, thereby improving oil adsorption capabilities. However, this treatment also resulted in reduced luminescence intensity and mechanical hardness, rendering the materials more flexible. Oleic acid modification enhanced the hydrophobic character of the material while improving compatibility between the filler and the polymer matrix.

Conclusion

This study successfully fabricated polyethylene-calcium carbonate (PE-CC) composites with tailored structural and surface properties to enhance oil adsorption. The composites were fabricated via melt blending using a 60/40 filler-to-polymer ratio, incorporating calcium carbonate (CC) modified with 0, 0.5, and 1.5 wt.% oleic acid (OA) to improve hydrophobicity. Subsequent citric acid (1 M) treatment induced porosity through partial dissolution of calcium carbonate, further refining the composite's performance. Structural characterization confirmed effective OA coating on CC, with XRD and FTIR analyses revealing reduced diffraction intensity and characteristic functional groups, indicating successful surface modification. XRD analysis of the composites verified the coexistence of PE and CC without chemical interaction, while the decrease in CC peak intensity after citric acid treatment of the PE-CC composites suggested partial CC dissolution. SEM imaging demonstrated uniform CC dispersion within the polymer matrix, with citric acid treatment creating voids up to 40 μm in TE 3, facilitating enhanced porosity. Elemental analysis supported this finding, showing calcium depletion after citric acid treatment. Surface roughness measurements indicated smoother profiles for citric acid-treated composites, while TE 3 exhibited moderate roughness with larger pores, improving adhesion and wettability. Wettability tests further reinforced this, showing increased hydrophilicity in citric acid-treated samples, enhancing water affinity. Photoluminescence analysis revealed blue-violet emissions with broad peaks centered at 405 and 570 nm under 255 and 405 nm excitation, respectively, suggesting potential optical applications. Oil adsorption studies indicated a significant increase in the uptake of both polar and non-polar liquids, particularly in TE 3, where higher porosity improved fluid retention. Shore hardness testing confirmed a reduction in material rigidity following citric acid and OA treatments, promoting flexibility without compromising structural integrity. These findings validate the chemical modifications employed in this study, demonstrating their effectiveness in enhancing porosity, surface interactions, and multifunctionality. The PE-CC composites have potential for environmental applications, particularly in oil remediation, where enhanced porosity and tailored surface properties are crucial for efficient adsorption and retention.

Funding

This research was supported by the African Union and the Pan African University Life and Earth Sciences Institute through a Ph.D. scholarship awarded to Ayodunmomi Esther Olowofoyeku.

Acknowledgments

Ayodunmomi Esther Olowofoyeku sincerely thanks the African Union and the Pan African University Life and Earth Sciences Institute for awarding a Ph.D. scholarship, which facilitated this research as a part of her doctoral research.

References

[1] S. Garg, Z.Z. Chowdhury, A.N.M. Faisal, N.P. Rumjit, and P. Thomas, Impact of Industrial Wastewater on Environment and Human Health, 2022, pp. 197-209.

[2] N. Singh, T. Poonia, S.S. Siwal, A.L. Srivastav, H.K. Sharma, and S.K. Mittal, Challenges of water contamination in urban areas, 2022, pp. 173-202.

[3] J. Kanungo, T. Sahoo, M. Bal, and I.D. Behera, Performance of Bioremediation Strategy in Waste Lubricating Oil Pollutants: A Review, Geomicrobiol. J. 41 (2024) 360-373.

[4] A.M. Hassan, E.W. Al-Shalabi, and M.A. Ayoub, Updated Perceptions on Polymer-Based Enhanced Oil Recovery toward High-Temperature High-Salinity Tolerance for Successful Field Applications in Carbonate Reservoirs, Polymers 14 (2022) 2001-2001.

[5] S.R. Benin, S. Kannan, R.J. Bright, and A. Jacob Moses, A review on mechanical characterization of polymer matrix composites & its effects reinforced with various natural fibres, Mater. Today: Proc. 33 (2020) 798-805.

[6] M. Ramesh, L.N. Rajeshkumar, N. Srinivasan, D.V. Kumar, and D. Balaji, Influence of filler material on properties of fiber-reinforced polymer composites: A review, e-Polymers 22 (2022) 898-916.

[7] J.-W. Zha, F. Wang, and B. Wan, Polymer composites with high thermal conductivity: Theory, simulation, structure and interfacial regulation, Prog. Mater Sci. 148 (2025) 101362-101362.

[8] S. Kartik Shubham, R. Purohit, P.S. Yadav, and R.S. Rana, Study of nano-fillers embedded in polymer matrix composites to enhance its properties – A review, Mater. Today: Proc. 26 (2020) 3024-3029.

[9] R.O. Ogunleye, and S. Rusnakova, A Review of Prestressed Fibre-Reinforced Polymer Matrix Composites, Polymers 14 (2021) 60-60.

[10] A. Shojaei, and S.S. Khasraghi, Self-healing and self-sensing smart polymer composites, Elsevier, 2021, pp. 307-357.

[11] R. Dweiri, Processing and Characterization of Surface Treated Chicken Eggshell and Calcium Carbonate Particles Filled High-Density Polyethylene Composites, Mater. Res. 24 (2021).

[12] F. Liendo, M. Arduino, F.A. Deorsola, and S. Bensaid, Factors controlling and influencing polymorphism, morphology and size of calcium carbonate synthesized through the carbonation route: A review, Powder Technol. 398 (2022) 117050-117050.

[13] N.M. Nurazzi, M.N.F. Norrrahim, M.H. Mulla, S.H. Kamarudin, M.S.A. Rani, A.I. Rushdan, and A.M. Kuzmin, Mechanical performance of seashell-reinforced polymer composites for structural applications, Elsevier, 2024, pp. 243-257.

[14] J. Qiu, J.W. Lyu, J.L. Yang, K.B. Cui, H.Z. Liu, G.F. Wang, and X. Liu, Review on Preparation, Modification and Application of Nano-Calcium Carbonate, Part. Part. Syst. Charact. 41 (2024) 1-12.

[15] S.C.S. Teixeira, M. M. Moreira, A.P. Lima, L.S. Santos, B.M. da Rocha, E.S. de Lima, R.A.A.F. da Costa, A.L.N. da Silva, M.C.G. Rocha, and F.M.B. Coutinho, Composites of high density polyethylene and different grades of calcium carbonate: Mechanical, rheological, thermal, and morphological properties, J. Appl. Polym. Sci. 101 (2006) 2559-2564.

[16] H. Xu, L. Yang, P. Wang, Y. Liu, and M. Peng, Kinetic research on the sorption of aqueous lead by synthetic carbonate hydroxyapatite, J. Environ. Manage. 86 (2008) 319-28.

[17] A. Homavand, D.E. Cree, and L.D. Wilson, Polylactic Acid Composites Reinforced with Eggshell/$CaCO_3$ Filler Particles: A Review, Waste 2 (2024) 169-185.

[18] A.E. Olowofoyeku, A.K. Aremu, A.O. Olorunnisola, A.E. Olowofoyeku, E.O. Faluyi, and D.G. Adekanmi, Photoluminescent Polymer Nanocomposites : Innovative Materials for Enhanced Light Management and Crop Yield Optimization, 9 (2025) 61-83.

[19] A. Patti, H. Lecocq, A. Serghei, D. Acierno, and P. Cassagnau, The universal usefulness of stearic acid as surface modifier: applications to the polymer formulations and composite processing, J. Ind. Eng. Chem. 96 (2021) 1-33.

[20] N.H. Aprilita, T. Febriani, P. Ofens, M. Nora, T.A. Nassir, E.T. Wahyuni, N. Sciences, and U.G. Mada, Conversion of the styrofoam waste into a high-capacity and recoverable adsorbent in the removing the toxic Pb^{2+} from water media, 26 (2024) 1-10.

[21] J. Wang, Z. Cheng, D. Chen, G. Li, J. Chen, K. Wang, L. Xu, and J. Huang, An injectable porous bioactive magnesium phosphate bone cement foamed with calcium carbonate and citric acid for periodontal bone regeneration, J. Mech. Behav. Biomed. Mater. 142 (2023) 105805.

[22] J. Fu, C.P. Leo, and P.L. Show, Recent advances in the synthesis and applications of pH-responsive $CaCO_3$, Biochem. Eng. J. 187 (2022) 108446-108446.

[23] A.H. Ritonga, B. Aritonang, G.E. Putri, K. Khairiah, E.W.B. Siahaan, and D. Meilani, PLA/LLDPE/Organo-Precipitated Calcium Carbonate Composites Containing LLDPE-g-OA Compatibilizers: Mechanical, Physical, Thermal, and Morphology, Indones. J Chem. 23 (2023) 1694-1703.

[24] D. Wang, H. Wang, B. Qian, H. Zou, K. Zheng, X. Zhou, Y. Song, and Y. Sheng, Preparation of hydrophobic calcium carbonate phosphors and its application in fluorescent films, J. Lumin. 219 (2020) 1-8.

[25] N. Thyashan, Y.S. Perera, R. Xiao, and C. Abeykoon, Investigation of the effect of materials and processing conditions in twin-screw extrusion, Int. J. Lightweight Mater. Manuf. 7 (2024) 353-361.

[26] H.M. Abd El-Lateef, M.M. Khalaf, M.F. Abou Taleb, and M. Gouda, Development of photoluminescent concrete from polystyrene plastic reinforced with electrospun polypropylene nanofibers, J. Photochem. Photobiol. A: Chem. 449 (2024) 1-9.

[27] ASTM, "Standard Test Method for Rubber Property—Durometer Hardness," *ASTM D2240-15(2021)*, ASTM International, 2021.

[28] ASTM, "Standard Test Method for Water Absorption of Plastics," *ASTM D570-22*, ASTM International, 2022.

[29] K. Longkaew, A. Gibaud, W. Tessanan, P. Daniel, and P. Phinyocheep, Spherical $CaCO_3$: Synthesis, Characterization, Surface Modification and Efficacy as a Reinforcing Filler in Natural Rubber Composites, Polymers 15 (2023).

[30] M. Al-Shirawi, M. Karimi, and R.S. Al-Maamari, Impact of carbonate surface mineralogy on wettability alteration using stearic acid, J. Pet. Sci. Eng. 203 (2021) 1-11.

[31] Y. Ma, P. Tian, M. Bounmyxay, Y. Zeng, and N. Wang, Calcium Carbonate@silica Composite with Superhydrophobic Properties, Molecules 26 (2021) 1-14.

[32] R. Beltrami, M. Colombo, G. Bitonti, M. Chiesa, C. Poggio, and G. Pietrocola, Restorative Materials Exposed to Acid Challenge: Influence of Temperature on In Vitro Weight Loss, Biomimetics 7 (2022) 30-30.

[33] A.K. Chaudhary, and R.P. Vijayakumar, Effect of chemical treatment on biological degradation of high-density polyethylene (HDPE), Environ. Dev. Sustainability 22 (2020) 1093-1104.

[34] A.H. Ritonga, N. Jamarun, S. Arief, H. Aziz, D.A. Tanjung, and B. Isfa, Improvement of Mechanical, Thermal, and Morphological Properties of Organo-Precipitated Calcium Carbonate Filled LLDPE/Cyclic Natural Rubber Composites, Indones. J Chem. 22 (2022) 233-241.

[35] B. Kanoje, J. Parikh, and K. Kuperkar, Crystallization study and morphology behaviour of calcium carbonate crystals in aqueous Surfactant-Pluronics® prototype, J. Mater. Res. Technol. 7 (2018) 508-514.

[36] A.H. Ritonga, N. Jamarun, S. Arief, H. Aziz, D.A. Tanjung, B. Isfa, V. Sisca, and H. Faisal, Organic modification of precipitated calcium carbonate nanoparticles as filler in LLDPE/CNR blends with the presence of coupling agents: impact strength, thermal, and morphology, J. Mater. Res. Technol. 17 (2022) 2326-2332.

[37] A. Aattache, and R. Soltani, Durability-related properties of early-age and long-term resistant laboratory elaborated polymer-based repair mortars, Constr. Build. Mater. 235 (2020) 117494-117494.

[38] P. Srihanam, W. Thongsomboon, and Y. Baimark, Phase Morphology, Mechanical, and Thermal Properties of Calcium Carbonate-Reinforced Poly(L-lactide)-b-poly(ethylene glycol)-b-poly(L-lactide) Bioplastics, Polymers 15 (2023) 301-301.

[39] F. Ippolito, G. Hübner, T. Claypole, and P. Gane, Influence of the Surface Modification of Calcium Carbonate on Polyamide 12 Composites, Polymers 12 (2020) 1295-1295.

[40] P. Zapata, H. Palza, B. Díaz, A. Armijo, F. Sepúlveda, J. Ortiz, M. Ramírez, and C. Oyarzún, Effect of $CaCO_3$ Nanoparticles on the Mechanical and Photo-Degradation Properties of LDPE, Molecules 24 (2018) 1-12.

[41] N. Hayeemasae, and H. Ismail, Potential of calcium carbonate as secondary filler in eggshell powder filled recycled polystyrene composites, Polímeros 31 (2021) 1-7.

[42] M. Gouda, H.M. Abd El-Lateef, M.F. Abou Taleb, and M.M. Khalaf, Photoluminescent polypropylene nanofiber-supported polyethylene terephthalate integrated with strontium aluminate phosphor, J. Photochem. Photobiol. A: Chem. 453 (2024) 1-9.

[43] M. Tareeva, M. Shevchenko, S. Umanskaya, V. Savichev, A. Baranov, N. Tcherniega, and A. Kudryavtseva, Two-Photon Excited Luminescence in Polyethylene and Polytetrafluoroethylene, J. Russ. Laser Res. 41 (2020) 502-508.

[44] T. Huang, K.D. Li, and M. Ek, Hydrophobization of cellulose oxalate using oleic acid in a catalyst-free esterification suitable for preparing reinforcement in polymeric composites, Carbohydr. Polym. 257 (2021) 117615.

[45] D. Jahani, A. Nazari, J. Ghourbanpour, and A. Ameli, Polyvinyl Alcohol/Calcium Carbonate Nanocomposites as Efficient and Cost-Effective Cationic Dye Adsorbents, Polymers 12 (2020) 2179-2179.

[46] N. Wierzbicka, R. Talar, K. Grochalski, A. Piasecki, W. Graboń, M. Węgorzewski, and A. Reiter, Influence of Inorganic Additives on the Surface Characteristics, Hardness, Friction and Wear Behavior of Polyethylene Matrix Composites, Materials 16 (2023) 4960-4960.

[47] D. Dey, and P. Banerjee, Toxic organic solvent adsorption by a hydrophobic covalent polymer, New J. Chem. 43 (2019) 3769-3777.